

Molar Heat Capacities, Thermodynamic Properties, and Thermal Stability of the Synthetic Complex $[\text{Er}(\text{Pro})_2(\text{H}_2\text{O})_5]\text{Cl}_3$

Xue-Chuan Lv,[†] Bei-Ping Liu,[‡] Zhi-Cheng Tan,^{*,†} Yan-Sheng Li,[§] Zhi-Heng Zhang,[†] Quan Shi,[†] Li-Xian Sun,[†] and Tao-Zhang[†]

Thermochemistry Laboratory, Dalian Institute of Chemical Physics, Chinese Academy of Science, Dalian 116023, China, Department of Chemistry, Hunan University of Arts and Science, Changde 415000, China, and College of Environmental Science and Engineering, Dalian Jiaotong University, Dalian 116028, China

The molar heat capacity, $C_{p,m}$, of a complex of erbium chloride coordinated with L-proline, $[\text{Er}(\text{Pro})_2(\text{H}_2\text{O})_5]\text{Cl}_3$, was measured from $T = 80$ K to $T = 400$ K with an automated adiabatic calorimeter. The temperature, the molar enthalpy, and the entropy of fusion and decomposition were calculated using equations and diagrammatic area integration. The thermodynamic functions $[H_T - H_{298.15}]$ and $[S_T - S_{298.15}]$ were derived from $T = 80$ K to $T = 360$ K with a temperature interval of 5 K. The thermal stability of the compound was investigated by differential scanning calorimetry and the thermogravimetric techniques.

Introduction

Rare earth elements have many unique properties and have been used in many areas, such as fertilizers, pesticides, antibacterial agents, and so on. As a result of such applications, rare earth elements are inevitably spread into the food chain and then into the bodies of human beings. To obtain information about the long-term effect of rare earth elements on people, the complexes of lanthanide ions with amino acids as ligands have been synthesized and extensively studied by a variety of methods.^{1–5} Only a few publications deal with thermodynamic investigations.^{6,7}

Molar heat capacities, $C_{p,m}$, of the compound at different temperatures are basic data in chemistry and engineering, from which many other thermodynamic properties can be calculated^{8,9} such as enthalpy, entropy, and Gibbs free energy, which are important for both theoretical and practical purposes. Only with thermodynamic data is it possible to quantitatively describe the energetic properties of substances such as thermal stability, stable forms at different temperatures, melting points, and energy changes in different processes.

In the present work, a complex of erbium chloride coordinated with L-proline, $[\text{Er}(\text{Pro})_2(\text{H}_2\text{O})_5]\text{Cl}_3$, was synthesized and characterized. A precision adiabatic calorimeter was used to measure the molar heat capacity, $C_{p,m}$, of the complex from $T = 80$ K to $T = 400$ K. In addition, the temperature, the molar enthalpy, and the entropy of fusion and decomposition were calculated using equations and diagrammatic area integration. At the same time, the thermodynamic functions, $[H_T - H_{298.15}]$ and $[S_T - S_{298.15}]$ were derived. The thermal stability of the compound was studied by the differential scanning calorimetry (DSC) and thermogravimetric (TG) techniques.

Experimental Section

Sample Preparation and Characterization. The title complex was prepared by the reaction of equimolar amounts of erbium

trichloride and L-proline in an aqueous solution at pH 4 for 8 h. The resulting solution was concentrated in a thermostat bath at 323 K until most of the water was evaporated. The concentrated solution was dried in a vacuum desiccator over phosphorus pentoxide for several weeks, and colorless crystals were obtained.

An elemental analysis apparatus (model PE-2400 II, USA) was used to measure the C, H, and N of the complex, and Er was determined by EDTA titration. Found: Er (28.10 %), C (20.20 %), N (4.75 %), and H (4.78 %), which is close to the theoretical values of Er (28.16 %), C (20.22 %), N (4.72 %), and H (4.75 %). The sample formula was determined to be $[\text{Er}(\text{Pro})_2(\text{H}_2\text{O})_5]\text{Cl}_3$, and the purity obtained from the EDTA titration under the same conditions was found to be 99.79 %.

Infrared spectra of the complex and L-proline were obtained from KBr pellets at room temperature using a Bruker Tensor 27 IR spectrophotometer. Compared with the IR spectrum of L-proline, the ν_s (carboxyl) band of the complex shifted from 1410 cm^{-1} to higher wavenumbers (1431 cm^{-1}), which shows that the carboxyl groups of the ligand have been coordinated to the metal ion.¹¹ The special absorptions of $-\text{NH}_2$ shifted from 3050 cm^{-1} to 3240 cm^{-1} ($\nu_{-\text{NH}}$), from 2750 cm^{-1} to 2740 cm^{-1} ($\nu_{-\text{NH}}$), and from 1560 cm^{-1} to 1562 cm^{-1} ($\delta_{\text{NH}_2^+}$) because a hydrogen bond formed in the complex. A broad absorption band for ν (hydroxyl) appearing at 3400 cm^{-1} shows the presence of water molecules in the complex.

Adiabatic Calorimetry. A precision automatic adiabatic calorimeter was applied to measure the heat capacity of the complex. The principle and structure of the instrument have been described in detail elsewhere.^{9,12–16} Briefly, the automatic adiabatic calorimeter was mainly composed of a sample cell, a miniature platinum resistance thermometer, an electric heater, the inner and outer adiabatic shields, two sets of six-junction chromel–constantan thermopiles installed between the calorimetric cell and the inner shield and between the inner and the outer shields, respectively, and a high vacuum can.¹⁴ The working temperature range is from $T = 78$ K to $T = 400$ K and where necessary can be cooled by liquid nitrogen. Prior to the heat capacity measurement of the sample, the molar heat

* Corresponding author. Fax: +86-411-84691570. E-mail: tzc@dicp.ac.cn.

[†] Chinese Academy of Science.

[‡] Hunan University of Arts and Science.

[§] Dalian Jiaotong University.

Table 1. Experimental Molar Heat Capacities ($C_{p,m}$) of $[\text{Er}(\text{Pro})_2(\text{H}_2\text{O})_5]\text{Cl}_3$

T K	$C_{p,m}$ $\text{J}\cdot\text{K}^{-1}\cdot\text{mol}^{-1}$	T K	$C_{p,m}$ $\text{J}\cdot\text{K}^{-1}\cdot\text{mol}^{-1}$	T K	$C_{p,m}$ $\text{J}\cdot\text{K}^{-1}\cdot\text{mol}^{-1}$	T K	$C_{p,m}$ $\text{J}\cdot\text{K}^{-1}\cdot\text{mol}^{-1}$	T K	$C_{p,m}$ $\text{J}\cdot\text{K}^{-1}\cdot\text{mol}^{-1}$	T K	$C_{p,m}$ $\text{J}\cdot\text{K}^{-1}\cdot\text{mol}^{-1}$
80.689	230.75	150.026	368.44	218.864	479.04	286.894	568.74	347.992	666.04	375.830	1570.5
84.765	239.28	152.917	372.31	221.856	482.90	289.811	573.65	351.023	667.92	376.065	1556.1
87.683	247.11	155.907	377.91	224.848	486.77	292.684	579.63	353.826	669.44	376.320	1545.8
90.700	253.59	159.000	383.40	227.879	489.70	295.544	584.48	356.250	670.26	376.599	1523.3
93.628	259.66	162.064	388.78	230.833	493.79	298.397	590.55	358.674	672.25	376.908	1518.9
96.479	265.69	165.103	393.60	233.826	498.48	301.212	593.91	361.212	673.42	377.231	1499.2
99.430	272.02	168.116	396.97	236.856	501.05	304.053	597.37	363.712	674.47	377.587	1477.1
102.480	278.51	171.103	401.82	239.811	505.04	306.848	602.58	366.176	674.55	377.998	1451.3
105.461	285.15	174.068	407.08	242.788	507.03	309.642	607.57	368.561	674.55	378.392	1426.5
108.382	290.24	177.011	411.74	245.758	510.07	312.415	613.48	370.188	674.55	378.846	1374.9
111.244	295.77	179.933	415.75	248.727	513.35	315.189	617.21	371.034	674.55	379.300	1323.3
114.209	302.62	182.833	420.64	251.629	516.28	318.001	623.84	371.746	674.55	379.754	1271.7
117.276	308.73	185.833	425.96	254.575	519.18	320.909	628.57	372.376	674.55	380.208	1220.1
120.288	313.82	188.930	430.98	257.487	523.15	323.758	633.49	372.940	674.55	380.662	1168.5
123.254	319.73	192.001	437.79	260.381	527.52	326.477	638.76	373.425	674.55	381.116	1116.9
126.176	325.71	195.053	445.10	263.258	530.52	329.129	644.26	373.830	674.55	381.570	1065.3
129.059	330.79	198.080	448.83	266.117	535.70	331.742	648.24	374.194	674.55	382.024	1013.7
132.043	336.58	201.085	453.82	269.061	540.59	334.508	651.17	374.455	674.55	382.478	962.1
135.129	341.75	204.072	458.49	272.088	543.81	336.932	653.63	374.742	674.55	382.932	910.5
138.176	347.02	207.038	462.50	275.093	548.27	339.280	657.49	374.996	674.55	383.386	858.9
141.186	352.77	209.811	466.86	278.084	552.23	341.591	659.95	375.205	674.55	383.840	807.3
144.163	358.23	212.788	471.19	281.052	556.31	343.939	661.48	375.396	674.55	384.294	755.7
147.108	362.74	215.879	474.47	284.015	562.30	346.098	664.52	375.602	674.55	384.748	704.1

capacities of $\alpha\text{-Al}_2\text{O}_3$, the standard reference material, were measured from $T = 78$ K to $T = 400$ K to verify the reliability of the adiabatic calorimeter. The results showed that the deviation of calibration data obtained in this work from those of NIST were within $\pm 0.3\%$ over the whole temperature range.

The heat capacity measurements were conducted by the standard procedure of intermittently heating the sample and alternately measuring the temperature. The heating rate and the temperature increments of the experimental points were generally controlled at 0.1 to $0.4\text{ K}\cdot\text{min}^{-1}$ and at 1 to 4 K. The heating duration was 10 min, and the temperature drift rates of the sample cell measured in an equilibrium period were kept within 10^{-3} – $10^{-4}\text{ K}\cdot\text{min}^{-1}$ during the acquisition of heat capacity data. The mass of $[\text{Er}(\text{Pro})_2(\text{H}_2\text{O})_5]\text{Cl}_3$ used for the measurement was 2.02791 g, which is equivalent to 0.0034 mol based on the molar mass $M = 593.58\text{ g}\cdot\text{mol}^{-1}$.

DSC and TG Techniques. Thermal analysis of $[\text{Er}(\text{Pro})_2(\text{H}_2\text{O})_5]\text{Cl}_3$ was performed using a differential scanning calorimeter (DSC-141, SETARAM, France) and a thermogravimetric analyzer (model DT-20B, Shimadzu, Japan).

The DSC was used with a heating rate of $10\text{ K}\cdot\text{min}^{-1}$ under high-purity nitrogen with a flow rate of $50\text{ mL}\cdot\text{min}^{-1}$. The mass of the sample used in the experiment was 3.01 mg. The calibrations for the temperature and heat flux of the calorimeter were performed prior to the experiment. The temperature scale was calibrated by measuring the melting points of Hg, In, Sn, Pb, and Zn at different heating rates, and the heat flux was calibrated using the Joule effect. Measurement of the melting temperature and the enthalpy of fusion of benzoic acid (NIST, SRM 39i) were made in this laboratory to check the accuracy of the instrument.

The TG measurement of the complex was undertaken at a heating rate of $10\text{ K}\cdot\text{min}^{-1}$ under high-purity nitrogen with a flow rate of $30\text{ mL}\cdot\text{min}^{-1}$. The mass of the sample used in the experiment was 9.70 mg. The reference crucible was filled with $\alpha\text{-Al}_2\text{O}_3$. The TG-DTG equipment was calibrated by the thermal analysis of the SRM, $\text{CaC}_2\text{O}_4\cdot\text{H}_2\text{O}(\text{s})$.

Results and Discussion

Molar Heat Capacity and Thermodynamic Functions. The experimental molar heat capacities, $C_{p,m}$, from $T = 80$ K to $T = 400$ K of $[\text{Er}(\text{Pro})_2(\text{H}_2\text{O})_5]\text{Cl}_3$ are presented in Table 1 and plotted in Figure 1.

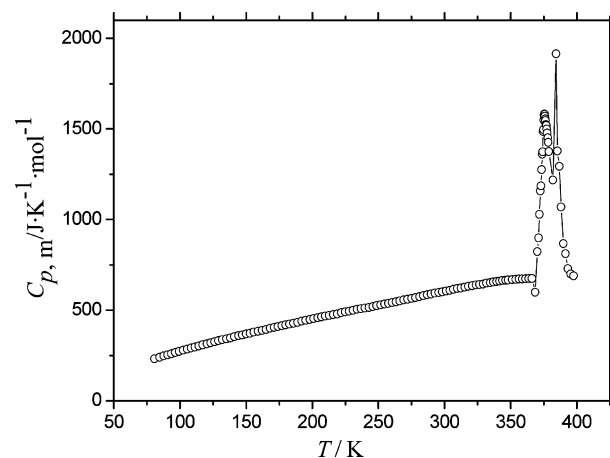


Figure 1. Experimental molar heat capacity plotted against temperature for the sample $[\text{Er}(\text{Pro})_2(\text{H}_2\text{O})_5]\text{Cl}_3$.

$= 400$ K of $[\text{Er}(\text{Pro})_2(\text{H}_2\text{O})_5]\text{Cl}_3$ are presented in Table 1 and plotted in Figure 1.

It can be seen from Figure 1 that the curve is continuous and smooth from $T = 80$ K to $T = 362$ K, which means that the structure of the complex is stable in the solid phase. From $T = 362$ K to $T = 397$ K, a peak occurs at 375.40 K, and another thermal anomaly appears at 384.40 K. The peak at $T = 375.40$ K was judged to be the melting process, which was consistent with a melting point $T = 375$ K as measured by the DSC. The thermal anomaly at 384.40 K, which only consists of three points, may be caused by the breakaway of the water molecules from the crystal lattice, consistent with the DSC and TG-DTG analysis.

A polynomial equation was obtained by least-squares analysis by using the experimental molar heat capacities ($C_{p,m}$) and the experimental temperatures (T). From $T = 80$ K to $T = 362$ K (solid phase), the equation is given as

$$C_{p,m}/(\text{J}\cdot\text{K}^{-1}\cdot\text{mol}^{-1}) = 483.13 + 214.04x - 15.045x^2 + 36.931x^3 + 13.72x^4 - 28.736x^5 - 30.926x^6 \quad (1)$$

where x is the reduced temperature, $x = [(T/\text{K}) - 221]/141$; T is the experimental temperature, the two constant values 221

Table 2. Thermodynamic Functions $[H_T-H_{298.15}]$ and $[S_T-S_{298.15}]$ of the Complex

T K	$C_{p,m}$ $J \cdot mol^{-1} \cdot K^{-1}$	$[H_T-H_{298.15}]$ $kJ \cdot mol^{-1}$	$[S_T-S_{298.15}]$ $J \cdot mol^{-1} \cdot K^{-1}$	T K	$C_{p,m}$ $J \cdot mol^{-1} \cdot K^{-1}$	$[H_T-H_{298.15}]$ $kJ \cdot mol^{-1}$	$[S_T-S_{298.15}]$ $J \cdot mol^{-1} \cdot K^{-1}$
80	228.64	-93.254	-510.56	230	496.74	-37.375	-141.74
85	240.51	-92.081	-496.33	235	504.27	-34.873	-130.97
90	251.89	-90.849	-482.27	240	511.79	-32.333	-120.27
95	262.87	-89.561	-468.37	245	519.32	-29.755	-109.64
100	273.49	-88.219	-454.63	250	526.85	-27.139	-99.066
105	283.82	-86.825	-441.05	255	534.40	-24.486	-88.555
110	293.89	-85.380	-427.62	260	541.98	-21.795	-78.103
115	303.73	-83.886	-414.34	265	549.60	-19.066	-67.705
120	313.37	-82.342	-401.22	270	557.25	-16.299	-57.361
125	322.84	-80.751	-388.23	275	564.93	-13.494	-47.067
130	332.16	-79.113	-375.38	280	572.65	-10.650	-36.821
135	341.34	-77.429	-362.67	285	580.40	-7.7668	-26.621
140	350.38	-75.700	-350.09	290	588.15	-4.8453	-16.465
145	359.31	-73.925	-337.64	295	595.91	-1.8849	-6.3509
150	368.13	-72.106	-325.31	298.15	600.78	0.0000	0.0000
155	376.84	-70.244	-313.10	300	603.63	1.1142	3.7224
160	385.44	-68.338	-301.00	305	611.30	4.1518	13.756
165	393.94	-66.389	-289.01	310	618.87	7.2275	23.750
170	402.34	-64.398	-277.13	315	626.29	10.3407	33.704
175	410.64	-62.366	-265.35	320	633.51	13.4906	43.617
180	418.85	-60.292	-253.68	325	640.45	16.6759	53.487
185	426.97	-58.177	-242.09	330	647.03	19.8951	63.311
190	435.00	-56.022	-230.61	335	653.16	23.1462	73.083
195	442.94	-53.827	-219.21	340	658.74	26.4265	82.798
200	450.80	-51.593	-207.90	345	663.63	29.7331	92.447
205	458.60	-49.319	-196.67	350	667.70	33.0622	102.02
210	466.32	-47.007	-185.53	355	670.79	36.4092	111.51
215	473.99	-44.656	-174.47	360	672.71	39.7688	120.89
220	481.61	-42.267	-163.48	360–390	melting range	melting range	melting range
225	489.19	-39.840	-152.57				

and 141 are obtained from the polynomials $(T_{max} + T_{min})/2$ and $(T_{max} - T_{min})/2$, respectively; T_{max} is the upper limit (362 K) of the above temperature region; and T_{min} is the lower limit (80 K) of the above temperature region. The correlation coefficient R^2 obtained from the least-squares fitting is 0.9999. The relative deviations of the smoothed heat capacities from those obtained from the experiment were within $\pm 0.3\%$.

The molar enthalpy and entropy of fusion, $\Delta_{fus}H_m$ and $\Delta_{fus}S_m$, of the compound were derived according to the following equations:

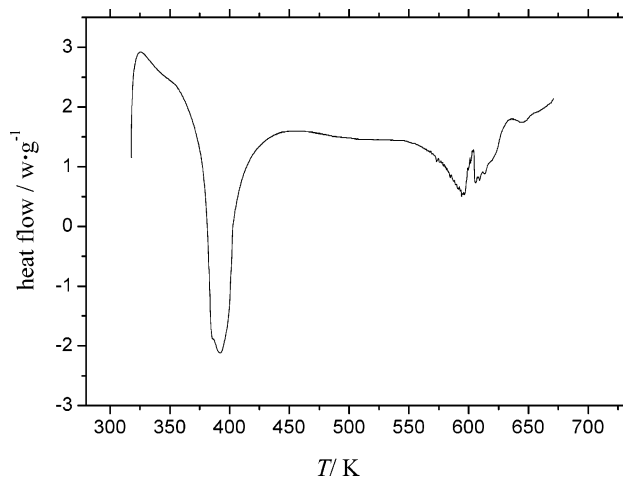
$$\Delta H_m = [Q - n \int_{T_i}^{T_m} C_p(s) dT - n \int_{T_m}^{T_f} C_p(l) dT - \int_{T_i}^{T_f} H_0 dT]/n \quad (2)$$

$$\Delta S_m = \Delta H_m/T_m \quad (3)$$

where T_i is the temperature a few degrees lower than the initial melting temperature, Q is the total energy introduced into the sample cell from T_i to T_f , T_f is a temperature slightly higher than the final melting temperature, $C_p(s)$ is the heat capacity of the sample in the solid phase from T_i to T_m , $C_p(l)$ is the heat capacity of the sample in liquid phase from T_m to T_f , and n is the molar quantity of the sample.

From these equations, the melting point, T_m , the molar enthalpy and the entropy of fusion, $\Delta_{fus}H_m$ and $\Delta_{fus}S_m$, for the synthetic complex were determined to be (375.40 ± 0.4) K, (255.34 ± 0.25) $kJ \cdot mol^{-1}$, and (680.17 ± 0.70) $J \cdot K^{-1} \cdot mol^{-1}$, respectively.

The molar enthalpy and entropy of decomposition, $\Delta_{dec}H_m$ and $\Delta_{dec}S_m$, of the compound were calculated by the diagrammatic area integration method. The decomposition point, T_d , the molar enthalpy, $\Delta_{dec}H_m$, and the entropy of decomposition, $\Delta_{dec}S_m$, for the synthetic complex were determined to be (384.40 ± 0.4) K, (47.79 ± 0.05) $kJ \cdot mol^{-1}$, and (124.32 ± 0.11) $J \cdot K^{-1} \cdot mol^{-1}$, respectively.

**Figure 2.** DSC curve of $[Er(Pro)_2(H_2O)_5]Cl_3$.

The thermodynamic functions $[H_T-H_{298.15}]$ and $[S_T-S_{298.15}]$ of the compound were calculated in the temperature range from $T = 80$ K to $T = 360$ K with a temperature interval of 5 K in terms of the polynomials describing the heat capacity and the thermodynamic relationships and have been listed in Table 2.

Thermal Analysis. The thermal analysis results of $[Er(Pro)_2(H_2O)_5]Cl_3$ are shown in Figures 2 and 3, respectively. The DSC curve (Figure 2) shows that the complex was stable before melting. The melting temperature of the sample was determined to be $T_m = 375.74$ K, which is in agreement with that obtained from the heat capacity measurements, 375.40 K. The enthalpy of fusion of the compound was determined to be 254.21 $kJ \cdot mol^{-1}$, in terms of the diagrammatic area integration by the computer, which is consistent with that obtained by adiabatic calorimetry, 255.34 $kJ \cdot mol^{-1}$.

The mass loss of $[Er(Pro)_2(H_2O)_5]Cl_3$ was mainly divided to two parts. Based on the TG curve and the structure of $[Er(Pro)_2-$

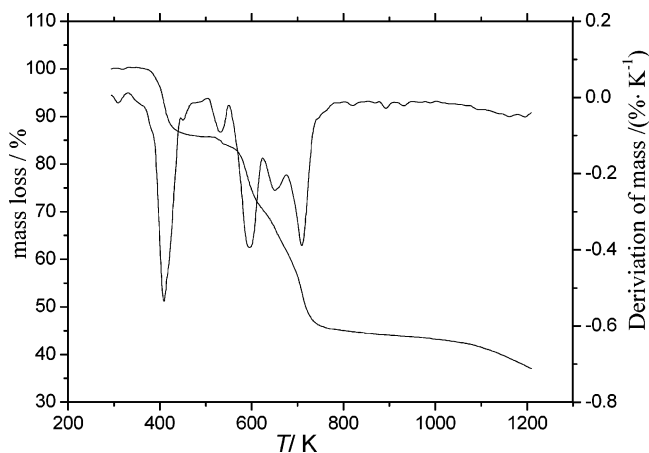
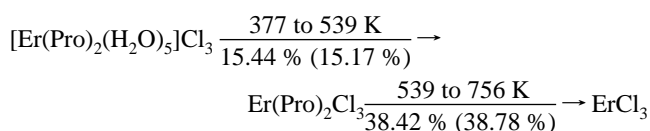


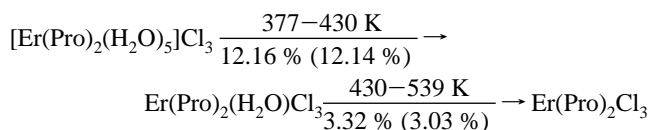
Figure 3. TG-DTG curve of $[\text{Er}(\text{Pro})_2(\text{H}_2\text{O})_5]\text{Cl}_3$.

$(\text{H}_2\text{O})_5]\text{Cl}_3$, the conclusion that can be drawn from $T = 377$ K to $T = 539$ K is that the five coordinating water molecules break away from the complex. The experimental mass loss (%) of the first step was found to be 15.44 %, a result that is consistent with the theoretical mass loss, 15.17 %, of the five water molecules. The second step of the mass loss from $T = 539$ K to $T = 756$ K should be due to the L-proline being separated from the Er^{3+} cations, and the residue of the TG experiment should be ErCl_3 . The experimental mass loss (%) of the decomposition is 38.42 %, which is again in accord with the theoretical mass-loss, 38.78 %.

The possible mechanism of the thermal decompositions was deduced as follows:



In the temperature range 377 K to 539 K, there are two stages of mass-loss of water molecules. The first is from 377 K to 430 K and constitutes the breaking away of the four water molecules. The mass loss found was 12.16 % in this range and compares well with the theoretical mass loss of 12.14 %. The second stage was deduced to be the losing of the last water molecule. The experimental mass loss (%) in this range, 3.23 %, is close to theoretical mass loss (%) of 3.03 %. The different loss order of water molecules was ascribed to the different status of these molecules in the complex:



Conclusion

In this work, the molar heat capacity, $C_{p,m}$, of a complex, $[\text{Er}(\text{Pro})_2(\text{H}_2\text{O})_5]\text{Cl}_3$, was measured from $T = 80$ K to $T = 400$ K using automated adiabatic calorimetry. The temperature, the

molar enthalpy, and the entropy of fusion and decomposition were calculated using equations and diagrammatic area integration. The thermodynamic functions $[H_T - H_{298.15}]$ and $[S_T - S_{298.15}]$ were derived from $T = 80$ K to $T = 360$ K with a temperature interval of 5 K. The thermal stability of the compound was investigated by the DSC and TG techniques. The possible mechanism of the thermal decompositions was deduced.

Literature Cited

- Zheng, Z. P. Ligand-controlled self-assembly of polynuclear lanthanide-oxo/hydroxo complexes: from synthetic serendipity to rational supramolecular design. *Chem. Commun.* **2001**, 2521–2529.
- Xu, H.; Chen, L. Study on the complex site of L-tyrosine with rare-earth element Eu^{3+} . *Spectrochim. Acta Part A* **2003**, *59*, 657–662.
- Wang, X. Q.; Jin, T. Z.; Jin, Q. R.; Xu, G. X. Synthesis of heteronuclear yttrium and lanthanide complexes with alanine; X-ray crystal structure of $[\text{ErY}(\text{Ala})_4(\text{H}_2\text{O})_8](\text{ClO}_4)_6$. *Polyhedron* **1994**, *13*, 2333–2336.
- Głowiak, T.; Legendziewicz, J.; Huskowska, E.; Gawryszewska, P. Ligand chirality effect on the structure and its spectroscopic consequences in $[\text{Ln}_2(\text{Ala})_4(\text{H}_2\text{O})_8](\text{ClO}_4)_6$. *Polyhedron* **1996**, *15*, 2939–2947.
- Csöreg, L.; Kierkegaard, P.; Legendziewicz, J.; Huskowska, E. Crystal Structure of apraseodymium glutamate perchlorate hydrate, $\text{Pr}_2(\text{L-Glu})_2(\text{ClO}_4)_4 \cdot 11\text{H}_2\text{O}$. *Acta Chem. Scand., Ser.* **1987**, *A41*, 453–460.
- Lan, X. Z.; Tan, Z. C.; Liu, B. P.; Nan, Z. D.; Sun, L. X.; Xu, F. Low-temperature heat capacity and thermal decomposition of crystalline $[\text{Er}_2(\text{His} \cdot \text{H}^+)(\text{H}_2\text{O})_8](\text{ClO}_4)_6 \cdot 4\text{H}_2\text{O}$. *Thermochim. Acta* **2004**, *416*, 55–58.
- Liu, B. P.; Tan, Z. C.; Lu, J. L.; Lan, X. Z.; Sun, L. X.; Xu, F.; Yu, P.; Xing, J. Low-temperature heat capacity and thermal decomposition of crystalline $[\text{RE}(\text{Gly})_3(\text{H}_2\text{O})_2]\text{Cl}_3 \cdot 2\text{H}_2\text{O}$ (RE = Pr, Nd, Gly = glycine). *Thermochim. Acta* **2003**, *397*, 67–73.
- Wang, S. X.; Tan, Z. C.; Di, Y. Y.; Xu, F.; Zhang, H. T.; Sun, L. X.; Zhang, T. Heat capacity and thermodynamic properties of 2,4-dichlorobenzaldehyde ($\text{C}_7\text{H}_4\text{Cl}_2\text{O}$). *J. Chem. Thermodyn.* **2004**, *36*, 393–399.
- Di, Y. Y.; Tan, Z. C.; Sun, X. H.; Wang, M. H.; Xu, F.; Liu, Y. F.; Sun, L. X.; Zhang, H. T. Low-temperature heat capacity and standard molar enthalpy of formation of 9-fluorene-methanol ($\text{C}_{14}\text{H}_{12}\text{O}$). *J. Chem. Thermodyn.* **2004**, *36*, 79–86.
- Ma, A. Z.; Li, L. M.; Lin, Y. H.; Xi, S. Q. Structure of an erbium coordination compound with L-proline, $\{[\text{Er}(\text{Pro})_2(\text{H}_2\text{O})_5]\text{Cl}_3\}_n$. *Acta Crystallogr.* **1993**, *C49*, 865–867.
- Nakamoto, K. *Infrared Spectra of Inorganic and Coordination Compounds*, 4th ed.; John Wiley & Sons: New York, 1986; 258 pp.
- Tan, Z. C.; Zhang, J. B.; Meng, S. H. A low-temperature automated adiabatic calorimeter. *J. Therm. Anal. Calorim.* **1999**, *55*, 283–289.
- Wang, M. H.; Tan, Z. C.; Sun, X. H.; Zhang, H. T.; Liu, B. P.; Sun, L. X.; Zhang, T. Determination of heat capacities and thermodynamic properties of 2-(chloromethylthio)benzothiazole by an adiabatic calorimeter. *J. Chem. Eng. Data* **2005**, *50*, 270–273.
- Tan, Z. C.; Sun, G. Y.; Sun, Y.; et al. An adiabatic low-temperature calorimeter for heat capacity measurement of small samples. *J. Therm. Anal.* **1995**, *45*, 59–67.
- Tan, Z. C.; Sun, G. Y.; Song, Y. J.; Wang, L.; Han, J. R.; Liu, Y. S.; et al. An adiabatic calorimeter for heat capacity measurements of small samples: the heat capacity of nonlinear optical materials KTiOPO_4 and RbTiOAsO_4 crystals. *Thermochim. Acta* **2000**, *252–253*, 247–253.
- Tan, Z. C.; Sun, L. X.; Meng, S. H.; Li, L.; Yu, P.; Liu, B. P.; Zhang, J. B. Heat capacities and thermodynamic functions of *p*-chlorobenzoic acid. *J. Chem. Thermodyn.* **2002**, *34*, 1417–1429.

Received for review December 13, 2005. Accepted May 28, 2006. This work was financially supported by the National Natural Science Foundation of China under NSFC Grant 20373072.

JE0505220